ELSEVIER

Journal of Chromatography A, 908 (2001) 49–70

JOURNAL OF CHROMATOGRAPHY A

www.elsevier.com/locate/chroma

Effect of the homogeneity of the column set on the performance of a simulated moving bed unit
I. Theory

Kathleen Mihlbachler[a,b,c], Jörg Fricke[a,d], Tong Yun[a,b], Andreas Seidel-Morgenstern[c], Henner Schmidt-Traub[d], Georges Guiochon[a,b,*]

[a]*Department of Chemistry, University of Tennessee, Knoxville, TN 37996-1600, USA*
[b]*Division of Chemical and Analytical Sciences, Oak Ridge National Laboratory, Oak Ridge, TN 37831-6120, USA*
[c]*Department of Chemical Engineering, O.-v.-Guericke University of Magdeburg, Magdeburg, Germany*
[d]*Department of Chemical Engineering, University of Dortmund, Dortmund, Germany*

Abstract

Although it is impossible to manufacture identical columns for use in a simulated moving bed (SMB) process, theoretical studies assume that all the columns in an SMB unit have identical characteristics. In practice, calculations in modeling and optimization studies are made with the average values of each column parameter set. In this report, the effects on SMB process performance caused by column-to-column fluctuations of the parameters are discussed. As a first step, we show how the differences in porosity of the columns may be taken into account with a revised set of separation conditions. Reductions in the purity of the extract and the raffinate streams are quantitatively related to the column-to-column fluctuations of the retention times of the two components arising from these porosity differences. For the sake of simplicity, the discussion first addresses the case of a four-column SMB operating under linear conditions. Then, the scope is extended to the cases of SMB units incorporating several columns in each section and to SMB units operating under nonlinear conditions. © 2001 Elsevier Science B.V. All rights reserved.

Keywords: Simulated moving bed chromatography; Retention factors; Porosity

1. Introduction

The simulated moving bed (SMB) process was invented by Broughton [1] in 1961, as an alternative to overcome many of the practical disadvantages of true moving bed (TMB) chromatography. It had proven practically impossible to move the solid phase through the column while achieving a reasonable column efficiency and not progressively eroding the solid-phase particles into dust. In contrast to TMB, the solid-phase movement in the SMB process is simulated by column switching. The process shown in Fig. 1 is not continuous, it is periodical. As a consequence, its properties are somewhat different from those of true counter-current process [2].

SMB is applied to several important industrial separations, especially the Sorbex [3] and Parex processes [4]. SMB is now attracting considerable interest as a continuous process implementing preparative chromatography for industrial separations in the pharmaceutical industry. The most promising

*Corresponding author. Department of Chemistry, University of Tennessee, Knoxville, TN 37996-1600, USA. Tel.: +1-865-974-0733; fax: +1-865-974-2667.

E-mail address: guiochon@utk.edu (G. Guiochon).

0021-9673/01/$ – see front matter © 2001 Elsevier Science B.V. All rights reserved.
PII: S0021-9673(00)00935-3

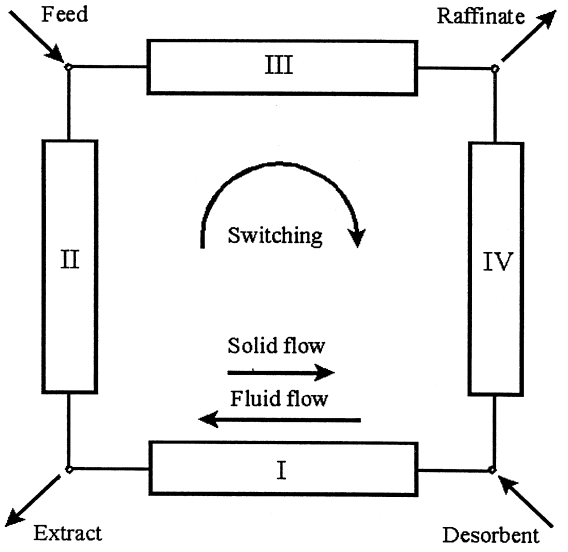

Fig. 1. Schematic of the SMB process.

application is the separation of enantiomers [5–9], a case in which the main disadvantage of the process disappears, its inability to separate mixtures in more than two fractions without using complex SMB implementations. Compared to the classical SMB applications in the chemical or food industry, enantiomeric separations are characterized by much smaller specific capacities of the adsorbents, lower values of the separation factors, and the absolute need to work under nonlinear conditions.

Most of the publications regarding SMB reported so far are devoted to discussions of its modeling, its properties, the optimization of its design and operation conditions, and to technical descriptions of either some new applications [10,11] or some improvements made on the classical implementation of the process [12–14]. On the theoretical front, besides the classical works of Rhee and Amundson [15], Ruthven and Ching [2], and Storti et al. [16,17], the reports by Fish et al. [18], Yun et al. [19], Zhong and Guiochon [20], and Mazzotti et al. [21] are worth noting. However, all fundamental discussions of SMB have so far assumed that all the columns have identical characteristics. Although the same batch of packing material may be used, it is impossible to manufacture four, let alone eight, 12, or 16 identical columns [22]. Therefore, in experimental analyses and optimizations, average values were applied.

The primary differences between columns arise from the practical impossibility to pack identical columns. The tubes may have slightly different geometric dimensions, leading to differences in the retention times at a constant flow-rate. These tubes may contain slightly different amounts of packing material, hence the retention factors of the feed components will also be different. More importantly, the packing procedure causes local fluctuations of the packing density which are highly irreproducible. Small relative variations of the local packing density, hence of the porosity, result in larger fluctuations of the permeability, hence the local mobile-phase velocity. Because the distribution of these differences is not reproducible, column-to-column variations of the porosity and permeability are observed. Even columns packed by axial compression with the same amount of the same packing material have slightly different retention times. The degree of reproducibility which can be achieved for the characteristics of small-size columns has been discussed previously [22]. Some of the effects of slight differences between the different columns were also reported previously [23]. The most notable was the observation of a superperiod for the composition of the column effluents, notably those of the raffinate and extract streams. This superperiod is the product of the basic SMB period and the total number of columns in the unit.

As far as the operation of an SMB separator is concerned, the most important fluctuations are those of the retention factors. In this first report, we discuss how variations in these factors for the two components of a binary mixture may affect the performance of an SMB. At this point, it is worth noting that other parameters, e.g. the column efficiency, may also have an important influence on the unit performance. However, we concentrate here on the porosity and assume that all the other parameters are kept constant.

2. Theory

The mathematical modeling of the SMB process includes three parts: the column model, the set of node equations, and the derivation of the proper separation conditions. The column model describes

the migration of the concentrations of the sample components along the column. It includes the conservation equations and their initial and boundary conditions, and the phase equilibrium of the two components between the liquid and the solid phases. The node equations are integral mass balance equations which must be fulfilled between the different sections of the SMB (or rather at its nodes). Finally, to reach complete separation of the feed mixture, a set of conditions has to be satisfied.

The modeling of the column introduces its characteristic properties. The most important one for the purpose of this work is the phase ratio, F. This ratio is a function of the total porosity of the packing material, ε, which is a critical operating parameter.

2.1. Porosity

The total porosity of the column is the fractional void volume of the column or proportion of the column volume that is occupied by the liquid phase. It is derived from the retention time, t_0, of a nonretained component:

$$\varepsilon_{\text{total}} = \frac{V_{\text{liquid}}}{V_{\text{column}}} = \frac{t_0 Q}{(\pi/4)(ID)^2 L_{\text{C}}} \tag{1}$$

where V_{column} and V_{liquid} are the volumes of the column and the liquid phase (or hold-up volume), respectively. The flow-rate Q is given by the experimental setting; to achieve it a certain head pressure is required. This pressure is usually limited by mechanical constraints. V_{column} is calculated from the known dimensions of the column tubing. V_{liquid} is the product of the flow-rate and the retention time of an unretained tracer. The retention time t_0 has to be corrected for the extra-column volumes (V_{extra}) contributed by tubings, valves, and online detectors. V_{extra} is measured similarly by substituting a zero-dead volume connector to the column.

The total porosity is the sum of the interparticle (external) ε_{ext} and the intraparticle (pore) porosity ε_{p} [24]. The pore porosity of a packing material is independent of the packing density achieved. The external porosity is the liquid volume outside the particles of packing material. It can be derived from the retention time or volume of a nonretained component which has a larger molecular size than the inlet diameter of the largest pores of the packing material [25]. The differentiation between internal and external porosity of the packing material is not needed in this work.

In this report, the word porosity is used instead of total porosity. As we see below, the porosity enters into the mass balance equation through the phase ratio, $F = (1 - \varepsilon)/\varepsilon$. Accordingly, relative fluctuations $\mathrm{d}\varepsilon/\varepsilon$ of the porosity will cause relative fluctuations of the phase ratio:

$$\frac{\mathrm{d}F}{F} = -\frac{\mathrm{d}\varepsilon}{\varepsilon} - \frac{\mathrm{d}\varepsilon}{1-\varepsilon} = -\frac{\mathrm{d}\varepsilon}{\varepsilon(1-\varepsilon)} \tag{2}$$

Since ε is usually between 0.65 and 0.80, the fluctuations of F will be several times larger than those of ε. This may have important consequences.

2.2. Column models

Two different column models are used in this work: the linear, ideal model and the equilibrium–dispersive model. The former model has exact algebraic solutions which can be used for the easy formulation of general conditions. These conditions, which do not take into account the band spreading caused by the finite column efficiency, can be corrected, using the numerical results afforded by the equilibrium–dispersive model.

2.2.1. Ideal model

The ideal model assumes instantaneous equilibrium between solid and liquid phases and an infinite column efficiency. Neglecting the contributions of axial dispersion and of the mass transfer resistances, the differential mass balance of component i (i = 1,2) in section j (j = I,II,III,IV) (see Fig. 1) is written

$$\frac{\partial C_{i,j}}{\partial t} + u_j \cdot \frac{\partial C_{i,j}}{\partial z} + F \cdot \frac{\partial q_{i,j}}{\partial t} = 0 \tag{3}$$

where $C_{i,j}$ and $q_{i,j}$ are the liquid- and solid-phase concentrations of component i in section j, respectively, u_j is the liquid-phase velocity in this section, and F is the phase ratio (see section above). An exact analytical solution of the linear, ideal model of SMB was derived previously [20]. This solution was shown to be a powerful tool in studying the thermodynamic limitations of SMB separations. An excel-

lent agreement was reported between the concentration profiles calculated with the analytical solution of the ideal model and the experimental results obtained in several cases [23,26], even with columns of moderate efficiency (a few hundred theoretical plates).

In this study, the porosity, hence the phase ratio, is not the same for all columns. The influence of this column characteristic must be included in the ideal model. Consequently, the mass balance of the component i ($i = 1,2$) in section j ($j = \mathrm{I,II,III,IV}$) and column k ($k = 1 \ldots$ total number of columns) is given as

$$\frac{\partial C_{i,j,k}}{\partial t} + u_{j,k} \cdot \frac{\partial C_{i,j,k}}{\partial z} + F_k \cdot \frac{\partial q_{i,j,k}}{\partial t} = 0 \tag{4}$$

2.2.2. Equilibrium–dispersive model

In contrast to the previous model, the axial dispersion and the mass transfer resistances are included in the equilibrium–dispersive model. However, the model assumes that the mass transfers are fast, so both effects are combined into an apparent dispersion coefficient, D_{ap}. To simplify the numerical calculations, we assume that the dispersion coefficient is independent of the components and constant in all the columns of the SMB unit. The differential mass balance for component i in section j and column k is then written

$$\frac{\partial C_{i,j,k}}{\partial t} + u_{j,k} \cdot \frac{\partial C_{i,j,k}}{\partial z} - D_{\mathrm{ap}} \cdot \frac{\partial^2 C_{i,j,k}}{\partial z^2} + F_k \cdot \frac{\partial q_{i,j,k}}{\partial t} = 0 \tag{5}$$

This model also assumes instantaneous and constant equilibrium between both phases, but it accounts for the effects of a finite column efficiency, N. Knowing the column efficiency, the apparent dispersion coefficient can be determined:

$$D_{\mathrm{ap}} = \frac{u_{j,k} L_{\mathrm{C}}}{2N_{j,k}} \tag{6}$$

where the mobile-phase linear velocity, $u_{j,k}$, depends on the porosity of the column, and on the section of the SMB in which the column is located. To ensure numerical stability in the calculation of the numerical solution of Eq. (5), the spatial increments in each column j,k have to be adjusted depending on the linear velocity, $u_{j,k}$, and the minimum efficiency, N_{min}.

This numerical solution of the model was proven accurate in many cases [6,27]. The model would have to be extended with a kinetic equation if the mass transfer kinetics is slow. Such a model, the transport–dispersive model [27], is not considered in this work.

2.3. Isotherm equation

The solid-phase concentration $q_{i,j,k}$ in Eqs. (4) and (5) is related to the mobile-phase concentration by the adsorption isotherm. A linear adsorption equilibrium is considered here, hence

$$q_{i,j,k} = f(C_{1,j,k}, C_{2,j,k}) = a_i C_{i,j,k} \tag{7}$$

Component 1 is assumed to be less retained than component 2 in the column, i.e. $a_1 < a_2$ and $\alpha = a_2 / a_1 > 1$.

In the case of nonlinear adsorption behavior, the relationship between solid and liquid phases can be described with the competitive Langmuir adsorption isotherm. This isotherm accounts for the competitive interactions of the feed components with the solid phase. If a common saturation capacity, q_{s}, is assumed, the isotherm model is thermodynamically consistent:

$$q_{i,j,k} = \frac{q_{\mathrm{s}} b_i C_{i,j,k}}{1 + \sum_{l=1}^{M} b_l C_{l,j,k}} \tag{8}$$

2.4. Initial and boundary conditions

To solve the mass balance equations, the correct initial and boundary conditions must be defined. The initial condition corresponds to a separator containing only the liquid and solid phases in equilibrium but no feed components:

$$C_{i,j,k}(x,0) = 0, \quad q_{i,j,k}(x,0) = 0 \tag{9}$$

The boundary conditions at the nodes between sections are defined as

$$\begin{aligned} C_{i,\mathrm{I},k}(0,t) &= \frac{C_{i,\mathrm{IV},k}(L_{\mathrm{C},t}) Q_{\mathrm{IV}}}{Q_{\mathrm{I}}} \\ C_{i,\mathrm{III},k}(0,t) &= \frac{C_{i,\mathrm{II},k}(L_{\mathrm{C},t}) Q_{\mathrm{II}} + C_i^F Q_{\mathrm{F}}}{Q_{\mathrm{III}}} \\ C_{i,j,k}(0,t) &= C_{i,j-1,k}(L_{\mathrm{C}},t), \quad j = \mathrm{II,IV} \end{aligned} \tag{10}$$

$$\frac{\partial C_{i,j,k}}{\partial z}(L_C,t) = 0 \quad (11)$$

The boundary conditions for additional columns in a section are equivalent to the third condition in Eq. (10). The inlet concentrations of a section are defined by the mass balance equations of the corresponding node. In the literature, the node model is described and discussed extensively [2,17,19,21,23,26]. This model combines the mass balance equation with the flow equation at each feed and draw-off node to realize the simulated counter-current in a series of columns. Note that the node model does not take into account the back-mixing and the dispersion which take place between columns, in the connecting tubes, valves, and pumps of the SMB separator. In practice, these parts contribute significantly to band dispersion. These contributions must be included in any theoretical modeling, particularly those of the dead volumes [28].

The feed and draw-off nodes are shifted, after a certain time equal to the SMB period, to the next position in the fluid direction. This creates the simulated counter-current motion of the solid phase. To account for this periodic changing of the feed and draw-off nodes, the boundary conditions of each column are updated accordingly at the beginning of each new cycle.

2.5. Conventional separation conditions

The successful operation of an SMB process relies on the fulfillment of a number of separation conditions. To achieve a good separation, the flow-rates in all four sections must be chosen in such a way that the fronts and rears of the bands of the two components of the feed are within specific location ranges at the end of each cycle. Ruthven and Ching [2] showed that an SMB separation can be studied as an equivalent TMB process when taking into account that the simulated solid-phase flow-rate of the SMB system is identical to the solid-phase flow-rate of the TMB process. This flow-rate is given by

$$Q_S = (1-\varepsilon_k)Au_S = (1-\varepsilon_k)AL_C/t^* \quad (12)$$

where t^* is the switching (or cycle) time, u_S the apparent velocity of the solid phase, and A the cross section of the column. The internal flow-rate of the TMB can be calculated by using

$$Q_j^{TMB} = Q_j^{SMB} - Q_S/F_k \quad (13)$$

The derivation of the separation conditions is based on the ideal or equilibrium model, i.e. on the assumption that axial dispersion and the mass transfer resistances are all negligible and that the column efficiency is infinite. In conventional studies of SMB, it is further assumed that the solid-phase flow-rate through each column and the void fraction of each column are the same. This assumption will no longer be valid if the columns have different characteristics, as we discuss later. In the linear case, the ratio of the internal flow-rate and the solid-phase flow-rate can be combined with the Henry coefficient by using a safety margin, β_j:

$$Q_I^{TMB}/Q_S = a_2\beta_I \quad (14)$$

$$Q_{II}^{TMB}/Q_S = a_1\beta_{II} \quad (15)$$

$$Q_{III}^{TMB}/Q_S = a_2/\beta_{III} \quad (16)$$

$$Q_{IV}^{TMB}/Q_S = a_1/\beta_{IV} \quad (17)$$

The flow-rate has to be larger in section III than in section II, since $Q_{III} = Q_{II} + Q_F$. Based on the safety margin this can be expressed by

$$\beta_{II}\beta_{III} < \alpha \quad (18)$$

To achieve the complete separation of a binary mixture in the framework of the ideal model (i.e., with no axial dispersion), the safety margins must be larger than one [2]:

$$\beta_j > 1 \quad (19)$$

Eqs. (18) and (19) define a sufficient number of criteria to allow the correct choice of the operating conditions in linear SMB. This set of conditions is equivalent to the one derived by Storti et al. [16] (see Appendix A), the so-called ''Triangle Theory''. However, both sets of conditions are based on the assumption that all columns have identical characteristics and an infinite efficiency. In practice, the different columns of an SMB separator cannot be identical. Their individual average porosity, per-

meability, retention factors, and their efficiency are more or less different, however slightly.

2.6. Revised set of separation conditions

When the columns ($k = 1, \ldots, n$) of an SMB have different properties, the true period of the system, the time after which the system returns to its initial conditions, is no longer the switching time but is n times larger. We call this time the superperiod of the SMB. When we consider an SMB with $n - 1$ identical columns, we define as the initial or first cycle of a superperiod the cycle during which the nth (i.e., the different) column is in the section considered. During the following cycles, this different column migrates progressively to the next sections, as usual.

As explained earlier, we focus in this work on the effects arising from columns having different porosities, hence different retention factors for the components of the feed. The retention factor of component i in the physical column k (a column which will be successively part of the four different sections of the SMB) is proportional to the Henry coefficient, a_i, and to the phase ratio, F_k. As discussed earlier, the phase ratio depends on the total porosity of the bed, ε_k. Both parameters are part of the equations used to calculate β_j (Eqs. (14)–(17)). Thus, the exact values of these important design parameters will vary from column to column. In some cases, it might even be that a $\beta_{k,j}$ is less than one during one of the cycles constituting the superperiod, while it will remain higher during the other cycles (or at least during most of them). The separation conditions derived above have to be extended to such cases. Every column leads to a different set of separation conditions. Thus, the total number of these conditions equals the total number of columns in the SMB process considered. Obviously, the characteristics of the production (amount produced per cycle and purity of both output streams) will vary during a superperiod.

Our first aim becomes the derivation of a revised set of separation conditions that allows the choice of the flow-rates through the four sections of an SMB process and takes into account the characteristics of the different columns used. By defining the dimensionless internal flow-rate as

$$r_j = \frac{Q_j t^*}{AL_C} \tag{20}$$

we can extend the separation conditions described above. In addition to r_j, we also define the following boundary parameters:

$$g_k = a_1(1 - \varepsilon_k) + \varepsilon_k \tag{21}$$

$$h_k = a_2(1 - \varepsilon_k) + \varepsilon_k \tag{22}$$

where the subscript k identifies the physical column. In Appendix B, we detail the derivation of the new separation conditions from the conditions given by Storti et al. [16,17]. A simple algebraic transformation leads to the following new set of equations:

$$r_I \geq h_k \tag{23}$$

$$g_k \leq r_{II} \leq r_{III} \leq h_k \tag{24}$$

$$r_{IV} \leq g_k \tag{25}$$

The important advantage of this extension compared to a method using the safety margins, β_j, and the ''Triangle Theory'' [16,17] is that r_j does not depend on the porosity of the columns. Thus, the operating conditions, which are described by the four internal flow-rates, do not change depending on the subset of physical columns contained in the section considered during a given cycle. Only the boundaries of the inequalities which define the conditions to be satisfied by the r_j's are functions of a_i and ε_k. These boundaries depend on the specific columns considered. As shown earlier [16,17], the constraints for the flow-rates in the central sections of the SMB unit (Eq. (24)) can be represented by a simple graph, the separation triangle. To achieve complete separation based on the equilibrium theory [15], the operating conditions must be chosen in such a way that the corresponding point in the (r_{II},r_{III}) plane is located inside a triangle defined by the parameters of the separation (see later and Fig. 2). Thus, when the columns are different, there is a different triangle in the (r_{II},r_{III}) plane for each column. For complete separation, the point representing the experimental conditions selected must be inside all these triangles. Since the production rate depends on the location of the point inside the triangle, variations between the

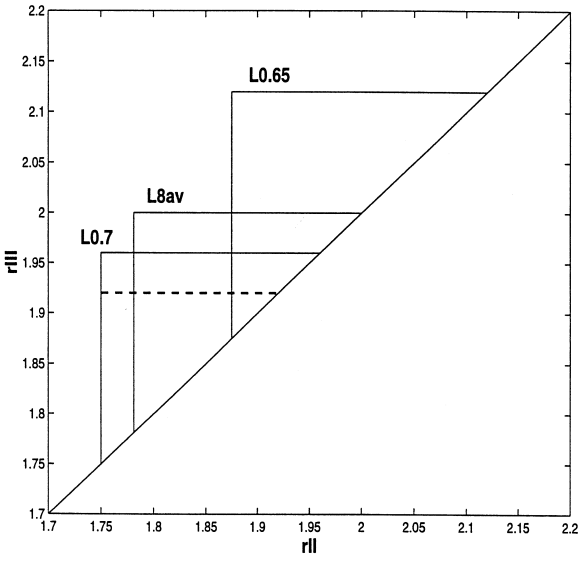

Fig. 2. Separation triangles based on the equilibrium theory for different porosities under linear conditions. Isotherm parameters: $a_1 = 3.5$ and $a_2 = 4.2$; solid line triangles — separation triangle for porosities of $\varepsilon = 0.7$ (L0.7) and $\varepsilon = 0.65$ (L0.65) and for the average porosity of eight columns of $\varepsilon = 0.6875$ (L8av); dashed line — horizontal scanning of the triangle ($r_{III} = 1.92$).

column characteristics will cause a change in the productivity of the unit considered.

In the following discussion, we examine only the effect of differences in the column porosity. Since the values of g_k and h_k are functions of both the Henry coefficients and the column porosities, this discussion is sufficient to describe the effect of different retention factors on the SMB process.

3. Results and discussion

In the following discussion, we need to use a specific example to illustrate the general results derived from the analytical solution of the ideal model under linear conditions and those obtained with the numerical solutions of the equilibrium–dispersive model under linear and nonlinear conditions. For this arbitrary example we elected a difficult separation, yet not uncommon for enantiomeric separations, with a separation factor $\alpha = 1.2$ and a Henry coefficient for the first component, $a_1 = 3.5$. The two additional coefficients b_1 and b_2 of the Langmuir equilibrium isotherm are 0.05 and 0.06 l/g, respectively. These coefficients guarantee a common saturation capacity.

For the sake of simplicity, we introduce in detail our revised set of conditions in the hypothetical case of a four-column SMB operated under linear conditions. In this case, a comparison is made between the analytical and numerical solutions. Later, we extend our discussion to multi-column SMBs (with two or more columns in each section). For the simulation the columns are assumed to be 10 cm long and to have a diameter of 1 cm. The calculations made under nonlinear conditions were performed with a feed concentration of 5 g/l for each compound.

In this study, one of the columns (called the *odd column* for the sake of convenience) has a different porosity $\varepsilon_1 = 0.65$ (hence $F_1 = 0.538$) while the other columns are identical and have a porosity $\varepsilon_2 = 0.70$ (hence $F_2 = 0.429$). Accordingly, the retention factors $k'_{1,k}$ and $k'_{2,k}$ of the two components are 1.883 and 2.26 on the odd, low-porosity column and 1.502 and 1.802 on the three high-porosity columns, respectively.

Note that the porosity difference selected (values of 0.65 versus 0.70) may seem to be large. Yet, it is realistic for a set of chromatographic columns packed carefully with the same material, at the same time, by the same operator [22]. Values of the relative standard deviation of 3.64, 2.55, and 2.07% are reported for four-, eight-, and 12-column systems, respectively. The chosen setting with only one column different from a set of identical columns is done for the sake of simplicity of this theoretical work.

Due to the cyclic nature of the SMB process, the odd column is successively substituted with one of the identical columns in each of the sections. In the next subsection, the observed changes in the concentration profiles of the two components in section II of the SMB are discussed for the linear case in detail. This discussion could also be done for section III. In either case, the concentration profile of only one product stream changes. Under linear conditions, the behaviors of the two sections can be studied independently because the linear isotherm is noncompetitive and there are no interactions between the concentration profiles of the two components.

3.1. Effect of different porosities under linear conditions

To achieve complete separation of the binary mixture and avoid contamination of one of the two products by the other one during all four cycles, the values chosen for r_{II} and r_{III} must fulfill the separation conditions (Eq. (24)) based on the equilibrium theory for all four columns. Thus, the point representing the chosen flow-rate ratios in Fig. 2 must lie inside the region common to the triangles labeled L0.65 and L0.7.

Obviously, the choice of the flow-rate in section II is limited by this new requirement. Points close to the apex of either triangles are excluded. Accordingly, the production rate decreases and the solvent consumption increases because the production rate is proportional to and the solvent consumption is inversely proportional to the distance between the operating point and the diagonal of the plot. If these points are inside the common area, close to the diagonal, the process has to be operated away from its optimum.

However, during part of the superperiod, the odd column is in either section I or section IV, where it does not contribute directly to the pollution of the product streams as long as the separation constraints are fulfilled in these sections (and solvent and solid phase are purified from feed components). Thus, there may be conditions under which the separation is degraded but not lost. We consider now operating points still located in the triangle L0.7 but outside the triangle L0.65 in Fig. 2. Under linear conditions, it is possible to identify several regions in this area. The mathematical derivation of these regions for a four-column SMB is presented in detail in Appendix C. Fig. 3 displays the boundaries of these regions for arbitrarily chosen values of $r_I = 2.2$ and $r_{IV} = 1.7$ which still satisfy the constraints of these two sections for all columns.

Within the first boundary ((1) dotted line, Eq. (C.8)), the separation condition in section II is not fulfilled during only one of the four cycles of the superperiod. The following cycle is able to compensate the variation of the column porosity. Accordingly, the extract stream is only polluted during this one cycle and is pure during the other three cycles. If the operating point is located within the boundary set by the dash-dotted line ((2), Eq. (C.13)), the cycle following the odd column could not push back the rear front of the raffinate entirely. The extract stream contains raffinate during two consecutive cycles. If the operating point is between the dash-dotted and the dashed line boundaries ((3), Eq. (C.17)), the extract is pure only during one cycle. Finally, the extract stream is polluted during all four cycles, to a different degree during each cycle, when the operating point is located outside this last boundary. However, the SMB process remains stable as long as the separation conditions are fulfilled in the first section. The higher flow-rate in section I prevents further pollution of the SMB system.

Fig. 3 shows a comparison between the different models describing the SMB process under linear conditions. At a constant value of $r_{III} = 1.92$, the separation area is scanned by changing r_{II} from the g_2-boundary (at $r_{II} = 1.75$, Eq. (21)) of the triangle L0.7 (Fig. 2) to the diagonal of the separation triangles ($r_{III} = 1.92$). The thick horizontal line in Fig. 3 represents the pure extract stream of the separation triangle calculated with the average porosity for a four-, eight-, and 12-column SMB system. These calculation are based on the equilibrium theory by neglecting axial dispersion and mass transfer resistance and assuming infinite efficiency. The thick line with dots displays the purity calculated using the analytical solution of the ideal model with four columns, with the exact porosity values. The purity of the extract stream declines significantly with decreasing r_{II}. There is a difference of approximately 2% at the boundary of g4av (separation triangle with an average porosity for four columns, Eq. (21)). The difference increases to approximately 6 and 10% at the boundaries of g8av and g12av, respectively.

The three thin lines with symbols represent the results of the numerical solution for the equilibrium–dispersive model with a minimal efficiency N_{min} of 100 plates to take the mass transfer and diffusion effects into account. The four-column SMB system (solid triangles) gives the largest difference from the ideal solution. The extract stream does not even reach 100% purity in the common area of both triangles (area between $g_1 = 1.875$, Eq. (21), and the diagonal). At the boundary of g12av, the extract is only 80% pure. Increasing the number of columns

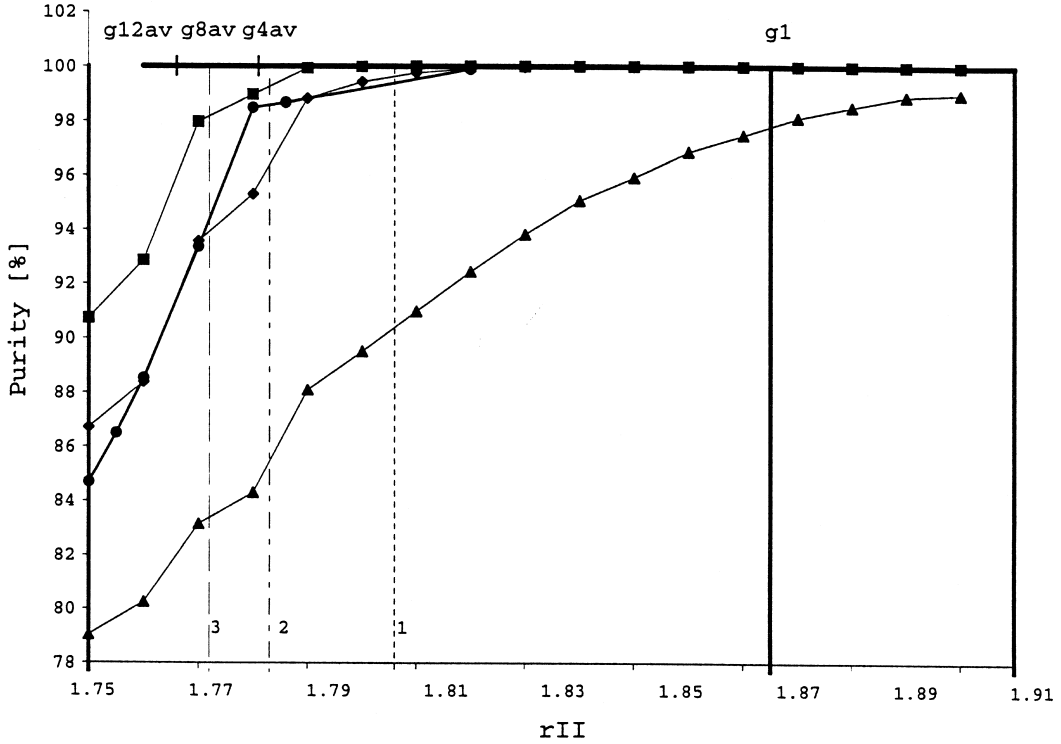

Fig. 3. Purity of the extract under linear conditions. Isotherm parameters, see Fig. 2; solid line — Eq. (21) with $g_1 = 1.875$ ($\varepsilon = 0.7$) and $g_2 = 1.75$ ($\varepsilon = 0.65$); thick solid line — pure extract based on ''Triangle Theory'' for average porosities of 12 (g12av), 8 (g8av), and 4 (g4av); column (1) dotted line — Eq. (C.8), (2) dash-dotted line — Eq. (C.13), (3) dashed line — Eq. (C.17); solid line with circle — analytical solution for four columns, solid line with square — 12 columns (100 plates), with diamond — eight columns (100 plates), and with triangle — four columns (100 plates).

per section results in a decrease of the influence of the single odd column. With two or more columns per section, the extract stream is pure within the common area. It is nearly so within the boundary of the dotted line. Of course, the purity of the extract is higher for three columns per section at lower r_{II} values. At the boundary of g12av, the extract is still approximately 95% pure, compared to approximately 89% with two columns per section. Choosing the operating conditions further inside the separation triangle reduces the differences more and more.

As shown with the simulation results under linear conditions, the influence of column-to-column variation can be corrected by using more than one column in section II. In an attempt to increase the production rate, the operating point may be selected outside the common area of the region defining complete separation for every single column in a four-column SMB unit. This will lead to pollution of at least one of the product streams. If the operating point lies left of the common area in Fig. 2, the concentration profile of component 1 does not entirely return past the feed node during the corresponding cycle. Therefore, the extract produced during the next cycle contains some component 1. By adding one or more columns into section II, the distance between the extract node and the rear end of the concentration band of component 1 can be increased. This minimizes the effect of axial dispersion and mass transfer kinetics and is the main reason why multi-column sections are frequent in SMB. The addition of a second column in section II can also reduce the consequences of column-to-column variations of the porosity or the retention factor (see Fig. 3). If the separation condition is not fulfilled during a cycle, the rear of the concentration band of com-

ponent 1 stays in the column next to the feed node at the end of the cycle. However, the extract steam is polluted only if the band profile is moved back into the first column of section II at the end of a cycle. This pollution can be avoided if the rear of the concentration band is entirely pushed back into one of the last columns of section II or in section III during the cycle that follows the one during which the separation condition is not satisfied. This arrangement requires that columns with a porosity higher than average be followed by columns with a porosity lower than average.

If the operating point is located above the area common to the operating triangles of all the columns, the concentration profile of component 2 passes the raffinate port during the cycle in which the column with the highest h_k is in section III and the raffinate stream of the second cycle will contain some component 2. If section III contains more than one column, however, the front of the band of component 2 may propagate through the first column after the feed node if this column has a higher than average porosity. However, in the additional column in section III, having a lower porosity, this front can be sufficiently pushed back toward the feed node during the next period. Then, pure raffinate can still be produced. This will happen if a column with a higher than average value of h_j is followed by a column with a value of h_j lower than average.

The modeling situation is more complex and the consequences less significant when the SMB unit contains several columns in some (or all) of its sections. An appropriate choice of the relative column positions may prevent pollution of the products. As the number of columns used in a section increases, the effect of column-to-column variations of their properties on the performance of the process decreases. It is the cycle-to-cycle fluctuations of the average set of p columns contained in the section that counts now, no longer the column-to-column fluctuations of the porosity. Obviously, the former is less than the latter.

Another option for limiting the effects of column-to-column variation is to take their arrangement into account. Since, in practice, all the columns will be different from the ''average'' one, is there a best way to position the columns relatively to each other when one has a set of columns of different porosities? Calculations were performed using all possible combinations of four different columns, all having different porosities. Our calculations did not find a significant difference between the performance of the SMB units made with different relative positioning of these columns, under linear conditions.

3.2. Influence of the separation factor on the acceptable column-to-column variations of the porosity

The consequences of having columns with different retention factors for the two feed components on the purity of the extract and raffinate were discussed in the previous section. It was shown that the ideal model predicts a separation of the feed into two streams of 100% pure products diluted into the desorbent only if the operating point lies inside the common area of the separation triangles defined by the different column characteristics. The more different the columns are from each other, the smaller this common area and the lower the production rate of pure fractions.

It would be useful to have a relationship estimating the maximum difference between the porosities of the odd column and that of the other three columns that allows the achievement of a certain separation, even with a zero production rate. We calculate here the maximum acceptable variation of the porosities of the individual columns around a constant average porosity, ε_{av}, for the set of columns used in an SMB unit. Following the equilibrium theory, the extract and the raffinate streams will be 100% pure if the operating triangles corresponding to the different columns overlap. The condition are fulfilled when the maximal value of the first boundary parameter, g_{max}, is smaller than the minimal value the second one, h_{min} (see Fig. 2). g_k and h_k are given by Eqs. (21) and (22). Because $a_i > 1$ in most cases, g_{max} corresponds to ε_{min} and h_{min} to ε_{max}. In this case, the acceptable limits of the porosity are $\Delta\epsilon/2$. A zero production rate is achieved if $g_{max} = h_{min}$. From Eqs. (21) and (22), the following relationship between α, a_1, and the average value of the porosity, ε_{av} is easily derived:

$$\frac{\Delta\varepsilon}{2} \leq \frac{(\alpha - 1)(1 - \varepsilon_{av})}{1 + \alpha - 2/a_1} \tag{26}$$

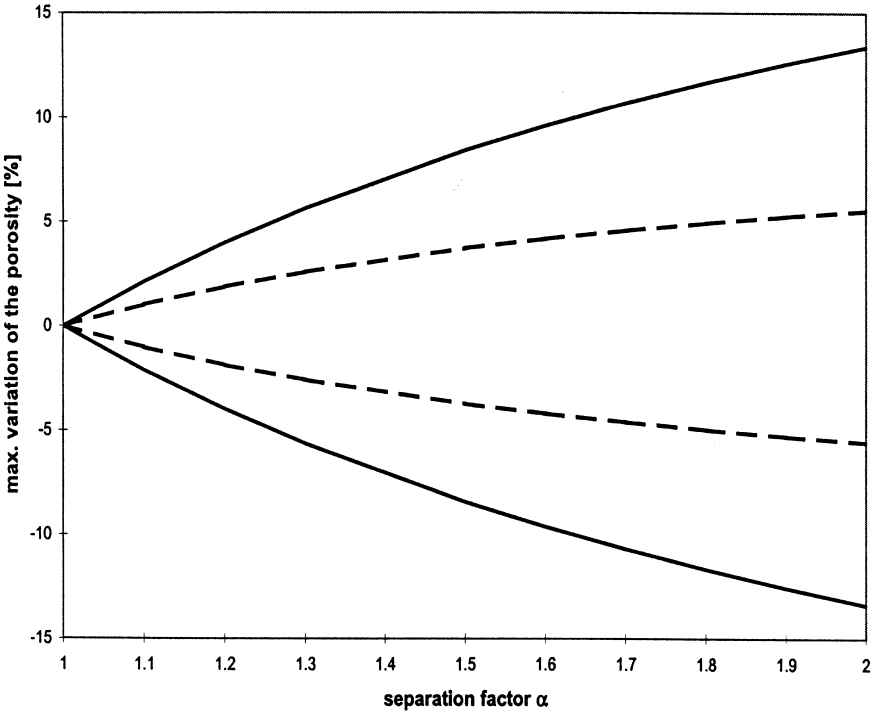

Fig. 4. Acceptable fluctuation of the porosity as a function of α. $\varepsilon_{av} = 0.675$ and $a_1 = 3.5$; solid line — zero production rate; dashed line — 50% production rate of the thermodynamic maximum.

This relationship is illustrated in Fig. 4. The acceptable relative variation of the column porosity increases with increasing separation factor. As α decreases, however, the areas of the triangles corresponding to the different columns decrease and their common area tends to vanish rapidly. Then, it becomes increasingly difficult to find an acceptable operating point. Eq. (26) must be used cautiously for several reasons.

First, the production rate is proportional to the distance of the operating point to the diagonal of the plot (Fig. 2), i.e. to the height of the triangle common to the operating triangles of all the columns [16,17]. The apex of the separation triangle corresponds to the maximum production rate. The latter is determined exclusively by the thermodynamics of the separation. When the common area vanishes, the production rate of nearly pure products (or, for that matter, of products of any given purity) decreases. Thus, pure products can be made along the solid lines in Fig. 4 but their production rate is zero, certainly an unacceptable situation. An important loss of production rate takes place for lower fluctuations of the column porosity. The figure shows that a porosity variation of $\pm 13\%$ is unacceptable even for very easy separations ($\alpha > 2.0$ and $a_1 = 3.5$) and variations of a few percent only are acceptable for $\alpha < 1.4$, a value that is not uncommon in enantiomeric separations. A more practical condition is also illustrated in Fig. 4. The dashed lines gives the porosity fluctuations which cause a 50% reduction of the maximum possible production rate, corresponding to the apex of the triangle L8av in Fig. 2. This limit can easily be calculated from simple geometrical relationships in this figure, leading to the following relationship:

$$\frac{\Delta\varepsilon}{2} = \frac{(a_1/2)(\alpha - 1)(1 - \varepsilon_{av})}{(a_1/2)(1 + 3\alpha) - 2} \tag{27}$$

This last result shows clearly how specifications regarding the acceptable column-to-column fluctuations should be set, based on the relationship between these fluctuations and the production rate loss

that they cause. A high production rate requires low variations of the column porosities.

Second, Eq. (26) is based on the ideal model and on a rigid assumption concerning the variation of the porosity from the average value. The influence of the finite column efficiency causes the profiles to become less steep and, accordingly, the production drop to become noticeable for lower variations of the column porosities but also to take place more progressively when the boundaries in Fig. 4 are approached. Admittedly, the apex of the L8av triangle is not a robust optimum and, for stability reasons as well as because of the axial dispersion of the band profiles, the operating points of SMB units should be located closer to the diagonal of the (r_{II},r_{III}) plot. This hardly changes anything essential to the rational just presented.

Finally, this discussion of the acceptable variations of the porosity in a set of columns is only valid under linear conditions. With increasing concentrations, the nonlinear behavior of the phase system increases and the common area of the now curvilinear separation triangles decreases very rapidly. So far, such a simple relationship as Eq. (26) could not be found for nonlinear separation. However, this relationship provides a good estimate of the minimum specifications required for satisfactory operation under moderately nonlinear conditions.

3.3. Effect of different porosities under nonlinear conditions

As mentioned earlier, the consequences of having SMB columns with different porosities become more severe under nonlinear conditions. Simple elution chromatograms calculated with our hypothetical Langmuir adsorption isotherm (Fig. 5) show significant variations of the retention times and band widths with changes in the column porosity. Both calculations were performed with the same values of the column efficiency ($N = 1000$), but for different porosities ($\varepsilon_1 = 0.65$ and $\varepsilon_2 = 0.7$). With a flow-rate of 1 ml/min the difference between the retention times is about 1 min. Due to the longer retention, the profile obtained with the lower-porosity column is somewhat broader than the one obtained with the high-porosity column.

Now, we examine the more realistic cases of a four-column and of multi-column SMB units operated under nonlinear conditions, with a feed at $C_{F,i} =$ 5 g/l, corresponding to $b_2 C_{F,2} = 0.30$, a relatively high degree of nonlinear behavior (see parameters at the beginning of the section Results and discussion). One of the columns is odd ($\varepsilon = 0.65$), the other have identical porosities ($\varepsilon_k = 0.70$). The calculations are performed using the same numerical solution algorithm of the equilibrium–dispersive model as used under linear conditions [6,27]. Calculations are carried out assuming column efficiencies of 30, 50, and 100 theoretical plates, successively. These efficiencies are typical of many current implementations of SMB under nonlinear conditions [29].

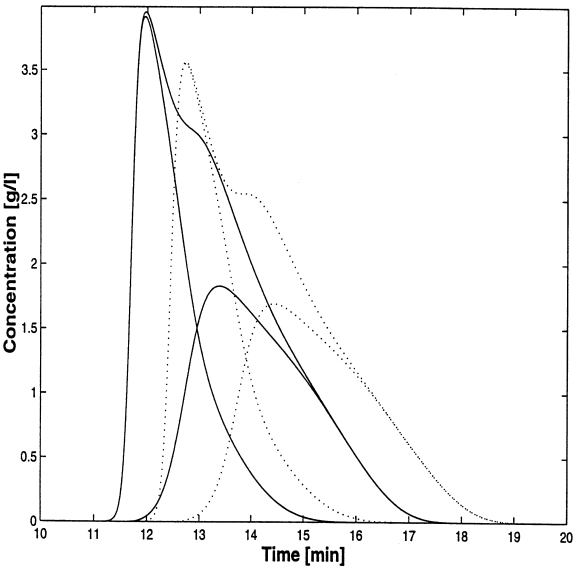

Fig. 5. Elution profiles of the competitive Langmuir Isotherm. Isotherm parameters: $a_1 = 3.5$, $a_2 = 4.2$, $b_1 = 0.05$, and $b_2 = 0.06$ with two different porosities ($\varepsilon_1 = 0.65$ — dotted line, $\varepsilon_2 = 0.7$ — solid line) for a concentration of 5 g/l and a flow-rate of 1 ml/min.

Fig. 6 shows the three separation triangles of the revised set of separation conditions, calculated [16] for both porosities and for the average porosity ($\varepsilon_{av} = 0.69375$) of an eight-column SMB, respectively. There are no reasonable operating conditions corresponding to the common area of the curvilinear triangles in Fig. 6. The feed flow-rate corresponding to the apex of this triangle ($F_{Feed} = 0.08$ ml/min for a switching time of 5.1 min) was smaller than the minimum flow-rate which our pump [9] can deliver

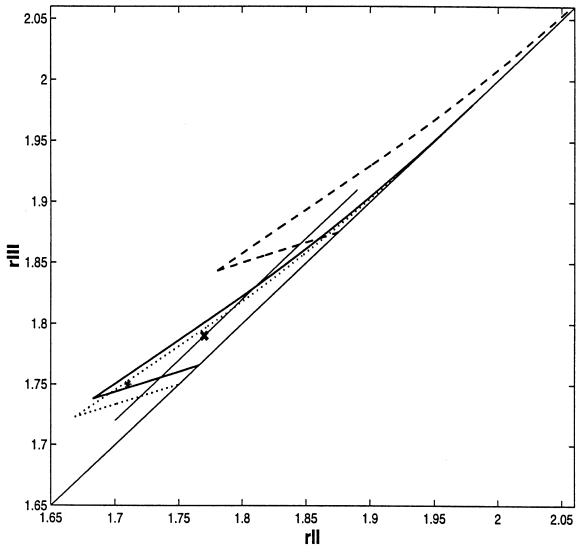

Fig. 6. Separation triangles based on the equilibrium theory for different porosities under nonlinear conditions ($C_{F,i} = 5$ g/l). Isotherm parameters: see Fig. 5; solid line triangle — separation triangles for eight-column SMB with an average porosity of $\varepsilon_{av} = 0.69375$; dashed line triangle — separation triangles for porosity $\varepsilon_1 = 0.65$; dotted line triangle — separation triangles for porosity $\varepsilon_2 = 0.7$; solid line — scanning the separation area parallel to the diagonal; operating point * — $r_I = 2$, $r_{II} = 1.71$, $r_{III} = 1.75$, and $r_{IV} = 1.6$; operating point × — $r_I = 2$, $r_{II} = 1.77$, $r_{III} = 1.79$, and $r_{IV} = 1.6$.

reproducibly. Thus, it was not possible to follow the same rational as used successfully earlier in this work, under linear conditions. As a first step we scanned the separation region parallel to the diagonal of the r_{II}–r_{III} diagram (solid line in Fig. 6). Calculations were performed assuming a column efficiency of 50 plates. Steady state was always reached after 200 cycles. The purities of the extract and raffinate obtained are displayed in Fig. 7. Parts (a), (b), and (c) of this figure correspond to results obtained for one, two, and three columns per section, respectively. The solid lines correspond to the boundaries of the separation triangles for the average porosities.

For the four-column SMB, the deviation between purities calculated with the exact porosity values and those obtained with the average porosity is most significant. At the operating point giving the purest product streams ($r_{II} = 1.77$ and $r_{III} = 1.79$, symbol × in Fig. 6), the extract purities calculated with the exact and the average porosities are 91.6 and 95.6% and those of the raffinate 88.6 and 92.05%, respectively (Fig. 7a). At the same operating point, the differences between the extract and raffinate purities calculated by the two methods decline to 0.5 and 0.6% for two columns per section, and to 0.03 and 0.09% for three columns per section, respectively.

The chromatograms of the eight-column SMB system corresponding to the operating point (×) are presented in Fig. 8. They were calculated for the 50-plate efficiency used in simulations discussed in Fig. 7b (thin line) and also for 30 plates (thick line), under steady-state conditions. These results illustrate the influence of the efficiency on the performance of the SMB. At the lower efficiency, the chromatograms obtained are more disperse and the product streams more polluted. The difference between the chromatograms calculated with the average porosity (eight identical columns) and the exact porosities (one odd, seven identical columns) is larger at lower plate numbers. In Table 1 the purities of the extract and raffinate are reported for the different conditions.

To increase the production rate of the SMB process, an additional operation point was chosen ($r_{II} = 1.71$ and $r_{III} = 1.75$, *). This point is much closer to the apex of the triangle of the average porosity (solid line in Fig. 6) but still inside the triangle of the higher-porosity column (dotted line). It corresponds to a higher flow-rate in section II than under the first condition. This leads to a higher production rate and a lower solvent consumption but also a less robust operation than under the first condition. In Table 2, the purity of the extract and the raffinate streams are reported. Again, this shows clearly that reducing the efficiency causes a decrease in product purity and also an increase in the difference between the stream purities calculated for a set of eight identical columns having the average porosity and for the actual set including an odd column and seven identical ones, even though both sets have the same average porosity. The difference between the purities of the two extract streams is significant for an efficiency of 30 plates (relative standard deviation of the average purity of the extract during each cycle over a superperiod, 2.09%). These results are illustrated by the chromatograms in Fig. 9 (column efficiencies, 30 and 100 plates). The thick line profiles ($N = 30$ plates) are broader and overlap more. The differences between the chromatograms

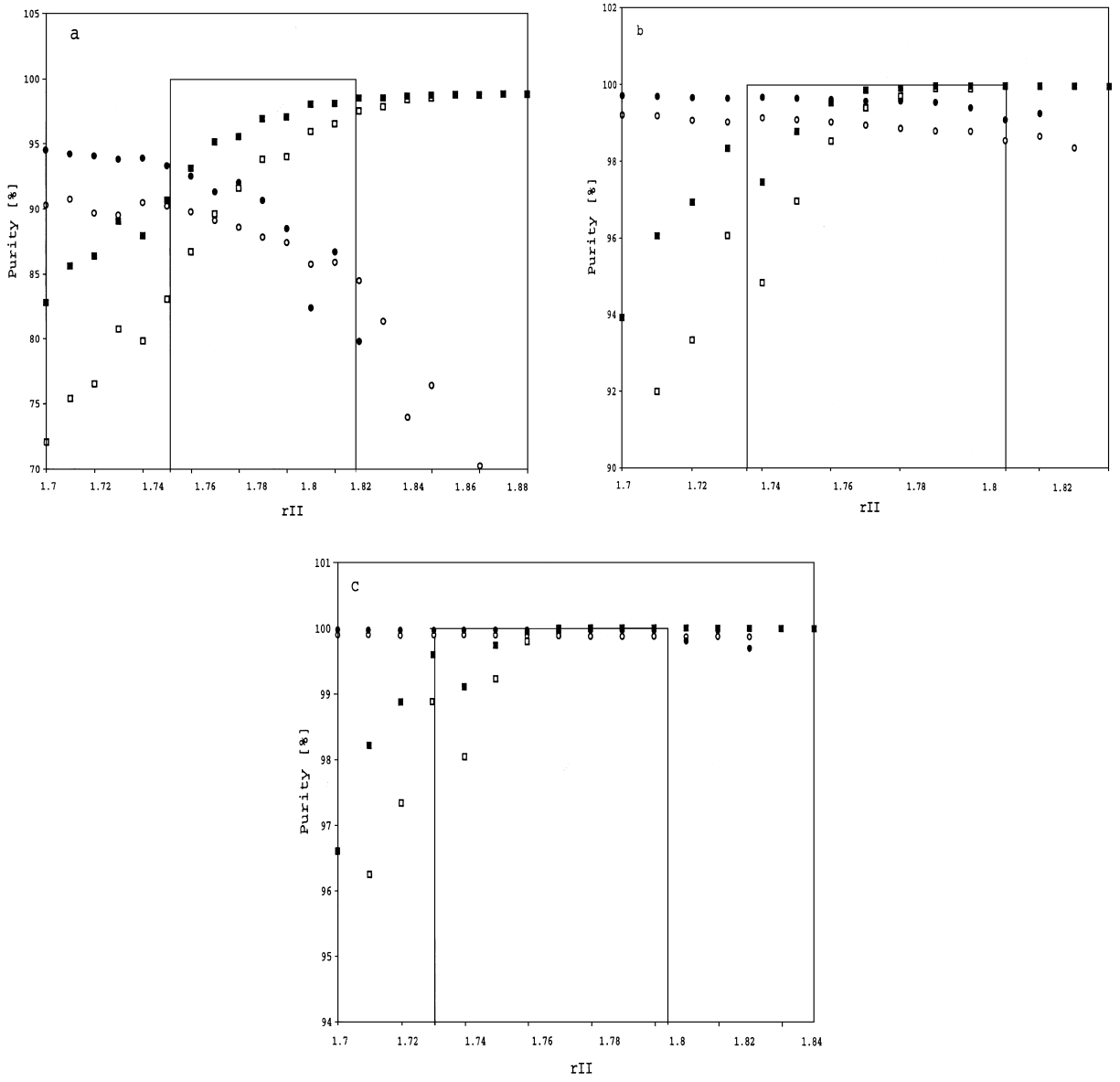

Fig. 7. Purities of the extract and raffinate under nonlinear conditions. (a) Four-column SMB, (b) eight-column SMB, and (c) 12-column SMB. operating point × — $r_{I} = 2$, $r_{II} = 1.77$, $r_{III} = 1.79$, and $r_{IV} = 1.6$. Isotherm parameters: see Fig. 5; solid line — separation area based on the ''Triangle Theory'' for the average porosity values; filled square — purity of the extract for the average porosities; empty square — purity of the extract for the exact porosities; filled circle — purity of the raffinate for the average porosities; empty circle — purity of the raffinate for the exact porosities.

calculated for the set of eight average-porosity columns (dotted line) and for the set of different columns (solid line) can be clearly seen.

Finally, the importance of considering the exact column characteristics is underlined by the results of a last calculation. In this case, we compare the results obtained with an eight-column SMB unit, using either eight identical columns of porosity $\varepsilon_{av} =$ 0.7 or a set of eight different columns all having different porosities (0.71, 0.66, 0.67, 0.71, 0.72,

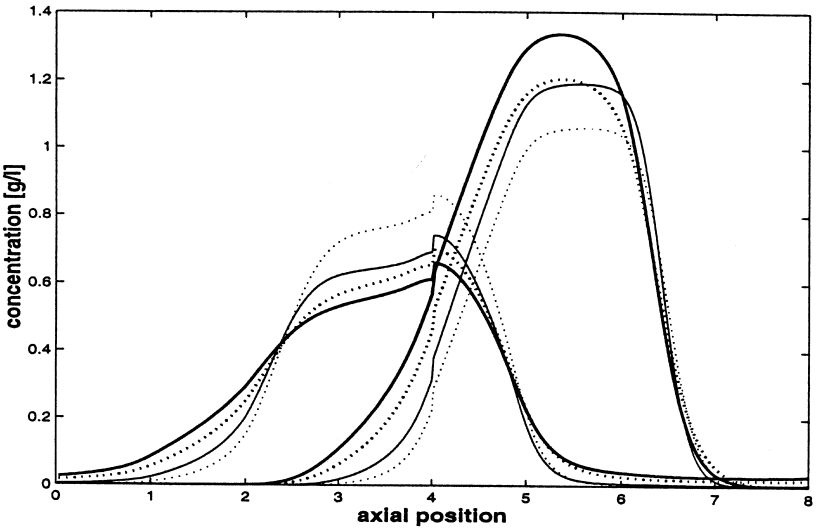

Fig. 8. Steady-state concentration profiles (200 cycles) of the separation condition (×) in Fig. 6. Isotherm parameters: see Fig. 5; solid line — seven columns with $\varepsilon_2 = 0.7$ and one column with $\varepsilon_1 = 0.65$; dotted line — eight columns with $\varepsilon_{av} = 0.69375$; thick line — 30 plates; thin line — 50 plates.

Table 1
Comparison of extract and raffinate purities calculated with the equilibrium–dispersive model at the operating point × in Fig. 6 ($r_I = 2$, $r_{II} = 1.77$, $r_{III} = 1.79$, and $r_{IV} = 1.6$) with different numbers of plates (50 and 30) under steady-state (200 cycles) and nonlinear conditions ($c_{F,i} = 5$ g/l)

Column	Number of plates			
number,	50		30	
k	Ex (%)	Ra (%)	Ex (%)	Ra (%)
1	99.31	98.98	93.71	94.37
2	99.35	98.99	93.94	94.44
3	99.38	99.00	94.15	94.48
4	99.41	99.00	94.32	94.51
5	99.43	98.89	94.48	93.96
6	99.45	98.92	94.62	94.08
7	99.47	98.94	94.74	94.20
8	99.49	98.98	94.85	94.30
Average purity value	99.41	98.96	94.35	94.29
Purity of ε_{av}	99.86	99.58	97.08	96.26
Difference	0.5	0.6	2.7	2
RSD (%)	0.19	0.44	2.02	1.46

Table 2
Comparison of extract and raffinate purities calculated with the equilibrium–dispersive model at the operating point * in Fig. 6 ($r_I = 2$, $r_{II} = 1.71$, $r_{III} = 1.75$, and $r_{IV} = 1.6$) with different numbers of plates (100, 50, and 30) under steady-state (200 cycles) and nonlinear conditions ($c_{F,i} = 5$ g/l)

Column	Number of plates					
number,	100		50		30	
k	Ex (%)	Ra (%)	Ex (%)	Ra (%)	Ex (%)	Ra (%)
1	99.29	99.88	98.08	99.35	92.61	97.27
2	99.33	99.88	98.17	99.35	92.86	96.07
3	99.37	99.88	98.25	99.36	93.08	96.08
4	99.40	99.88	98.32	99.36	93.26	96.09
5	99.43	99.87	98.38	99.32	93.41	95.86
6	99.45	99.88	98.43	99.33	93.55	95.91
7	99.47	99.88	98.47	99.33	93.67	95.97
8	99.49	99.88	98.51	99.34	93.77	96.01
Average purity value	99.40	99.88	98.33	99.34	93.28	96.00
Purity of ε_{av}	99.94	99.99	99.42	99.73	96.08	97.27
Difference	0.6	0.1	1.1	0.4	2.8	1.3
RSD (%)	0.38	0.08	0.78	0.28	2.09	0.93

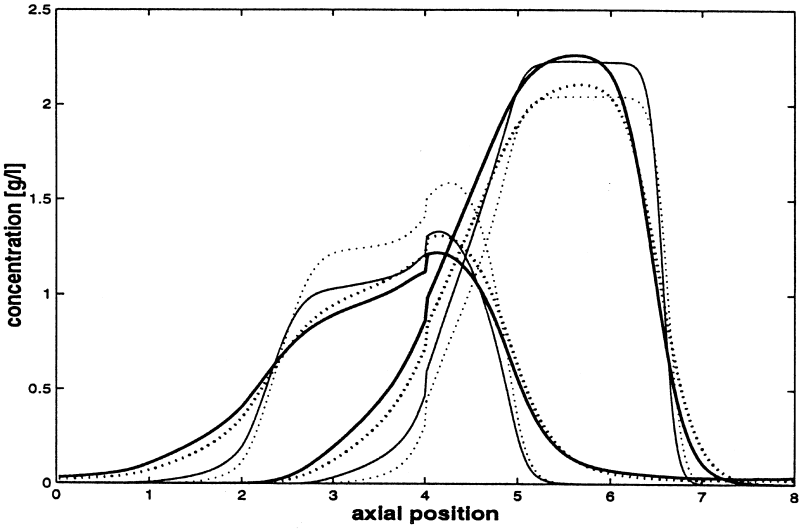

Fig. 9. Steady-state concentration profiles (200 cycles) of the separation condition (*) in Fig. 6. Isotherm parameters: see Fig. 5; solid line — seven columns with $\varepsilon_2 = 0.7$ and one column with $\varepsilon_1 = 0.65$; dotted line — eight columns with $\varepsilon_{av} = 0.69375$; thick line — 30 plates; thin line — 100 plates.

0.68, 0.77, and 0.69) randomly generated by the Microsoft Excel Tool. For this last set the mean value is 0.7 and the relative standard deviation 5%. The calculations were performed with a column efficiency of 50 plates, under the same experimental conditions of the first operating point (*). In Fig. 10, the solid and the dotted lines show the calculated band profiles. The difference between the extract purities is 1%. Regaining this extra 1% purity could be costly in terms of production rate in some cases.

Table 3 reports the production rates obtained with the two column sets. The production rates of the

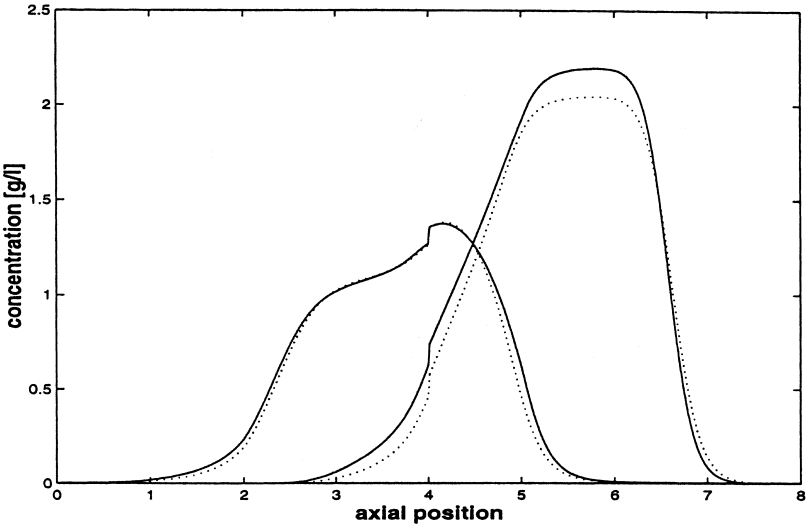

Fig. 10. Comparison of the steady-state concentration profiles (200 cycles) of the separation condition (*) in Fig. 6 for an average porosity of $\varepsilon_{av} = 0.7$ (dotted line) and eight different porosities ε_k (0.71, 0.66, 0.67, 0.71, 0.72, 0.68, 0.77, and 0.69) (solid line). Isotherm parameters: see Fig. 5.

Table 3
Production rate of extract and raffinate calculated by the equilibrium–dispersive model at the operating point * for conditions defined in Fig. 10

k	Production rate (10^{-5} mg/s ml_{pack})	
	Extract	Raffinate
1	9.5	9.9
2	9.6	10.6
3	9.6	9.4
4	9.7	10.0
5	9.4	9.7
6	8.6	9.4
7	9.7	9.7
8	9.3	9.5
Average PR value	9.4	9.8
RSD (%)	3.8	4.1
PR of ε_{av}	9.4	9.3

extract and the raffinate are functions of the average concentration of the requested component, the extract or the raffinate flow-rates, and the total volume of packing material in the set of columns. There is no significant difference between the extract production rates of both systems but the difference between the production rates of the raffinate has an RSD of 3.7%. During the eight cycles of the superperiod, the values of the production rates of the extract and raffinate are also changing, with RSDs of 3.8 and 4.1%, respectively.

4. Conclusion

Several important conclusions can be drawn regarding the influence of column-to-column fluctuations of the porosity on the production rate and product purity which can be achieved under linear and nonlinear conditions.

(1) The requirement usually set in theoretical studies of SMB that all the columns are identical is set for convenience. A SMB unit can be operated successfully with columns giving significantly different retention times for the two compounds involved in the separation. The consequences of using different columns in a SMB unit may be serious.

(2) The specifications regarding the acceptable range of parameters for the different columns of a SMB unit become more severe when the separation factor decreases. They become drastic when α approaches 1. This increased severity of the requirement of narrow fluctuations of the column characteristics may eventually limit the applicability of the SMB process in the case of really difficult separations (α around or below 1.1).

(3) The closer to the optimum are the conditions under which this process is operated, the more the production rate and/or the product purity decrease with increasing fluctuations of the column characteristics.

(4) SMB implementations using more than one column in a section are more robust toward column-to-column variations of the column properties than the equivalent ones having only one column per section. The robustness increases with increasing number of columns in each section.

(5) There is only a minor influence of the column arrangement on the performance of an SMB. A barely significant compensation of the effects of column-to-column variations is achieved by alternating the columns, juxtaposing columns with extreme characteristics.

(6) The results of this study can be extended to SMB separation operated under nonlinear conditions. The effect of the nonlinear behavior of the isotherm can be illustrated easily using r_j (Eq. (20)) to define the separation conditions. If the isotherm is nonlinear and the feed concentration increases, the region of complete separation becomes smaller. It is no longer a rectilinear but a curvilinear triangle. If the columns are different, each one of them has a different curvilinear triangle. In order to achieve a high product purity, the operating point must be located inside the triangle corresponding to N identical columns having the average porosity but not too close to its apex or its borders (the last condition arises from the need to use columns with a finite efficiency). Calculations show that the area available decreases with increasing amplitude of the column-to-column variations. Since the area of a separation triangle is already smaller under nonlinear than under linear conditions, the specifications regarding columns are most important in the case of difficult, nonlinear separations, e.g. many enantiomeric ones. Careful attention must be paid to setting and enforc-

ing proper specifications for the range of variations of the column properties.

(7) Finally, although emphasis was placed in this work on column-to-column fluctuations of the column porosity, the influence of any other parameter that controls the retention times or the migration velocity associated with any given concentration of the two solutes will be similar. For large columns, the batch-to-batch reproducibility of designer packing material (e.g., for enantiomeric separations) may become a critical issue [30].

5. Nomenclature

a	Henry isotherm coefficient
A (cm^2)	column cross section
C (g/cm^3)	liquid-phase concentration
D_{ap} (cm^2/s)	axial dispersion coefficient
F	phase ratio
g	amount of component 1 per volume and unit concentration
h	amount of component 2 per volume and unit concentration
I.D. (cm)	internal diameter of the column
L_C (cm)	column length
N	theoretical number of plates
PR ($mg/s\ ml_{pack}$)	production rate of component 1 or 2
q (g/cm^3)	solid-phase concentration
Q (cm^3/s)	flow-rate
r	dimensionless flow-rate
t (s)	time
t^* (s)	switching time
u (cm/s)	liquid-phase flow velocity
z	axial coordinate

5.1. Greek symbols

α	separation factor
β	margin parameter
ε	overall void fraction

5.2. Subscripts

D	desorbent
E	extract
F	feed
R	raffinate
S	solid
i	feed component ($i = 1,2$)
j	section (I, II, III, IV)
k	number of columns
max	maximal value of g (see above)
min	minimal value of h (see above)
p	pore or particle

Acknowledgements

This work was supported in part by grant CHE-00-70548 of the National Science Foundation and by the cooperative agreement between the University of Tennessee and the Oak Ridge National Laboratory. The scholarship of the ''Martin-Schmeisser-Stiftung'' financially supported J.F. during his stay at the University of Tennessee, Knoxville.

Appendix A. Comparison of two separation conditions

The two leading theories of complete separation in SMB are the safety margin approach [2,23] and the ''Triangle Theory'' [16,17,21]. Both approaches are based on the equilibrium theory and can be transformed into each other [31]. Eqs. (14)–(17) in the main text result from the first of these two theories. Rewriting them with the classical relationship $Q_j^{TMB} = Q_j^{SMB} - Q_S/F$ leads to the following equations for the SMB process:

$$Q_I^{SMB}/Q_S - 1/F = a_2\beta_I \quad (A.1)$$

$$Q_{II}^{SMB}/Q_S - 1/F = a_1\beta_{II} \quad (A.2)$$

$$Q_{III}^{SMB}/Q_S - 1/F = a_2/\beta_{III} \quad (A.3)$$

$$Q_{IV}^{SMB}/Q_S - 1/F = a_1/\beta_{IV} \quad (A.4)$$

The left-hand sides of these last four equations are identical to the corresponding ratios of the net fluid flow-rate and the adsorbed phase flow-rate m_j. These ratios are used as the basis for the separation conditions of the ''Triangle Theory'' in the following equations:

$$a_2 < m_1 < \infty \tag{A.5}$$

$$a_1 < m_2 < a_2 \tag{A.6}$$

$$a_1 < m_3 < a_2 \tag{A.7}$$

$$-\frac{\varepsilon_p}{1-\varepsilon_p} < m_4 < a_1 \tag{A.8}$$

where m_2 has to be larger than m_3 because the flow-rate must be larger in section III than in section II. Substituting m_2 and m_3 in this last condition ($m_2 > m_3$) with the equivalent expressions $a_1\beta_{II}$ and a_2/β_{III}, respectively, gives directly $a_1\beta_{II} > a_2/\beta_{III}$, i.e. Eq. (18) ($\beta_{II}\beta_{III} < \alpha$). Similarly, if m_j in Eqs. (A.5)–(A.8) is replaced by the corresponding expressions using a_i and β_j then the condition presented in Eq. (19) ($\beta_j > 1$) is fulfilled.

If we choose β_{IV} greater than one, $m_{IV} = a_1/\beta_{IV}$, which is positive, and cannot be smaller than the negative limit value given by Eq. (A.8). The void fraction inside the particle ε_p in this equation can be neglected, and the lower limit is zero.

In conclusion, the two sets of operating conditions were proven to be equivalent.

Appendix B. Derivation of revised separation conditions

The revised set of separation conditions can be derived directly from the relationships derived in Appendix A and given in Eqs. (A.5)–(A.8) and from the condition $m_2 < m_3$ [21]. The value m_j is defined as [21]

$$m_j = \frac{Q_j^{SMB}t^* - V\varepsilon}{V(1-\varepsilon)} = \frac{Q_j^{SMB}t^*}{V(1-\varepsilon)} - \frac{\varepsilon}{1-\varepsilon} \tag{B.1}$$

where t^* is the switching time and V is the total volume of the column. Eq. (B.1) can be rewritten for columns having different porosities ε_k:

$$m_j = \frac{Q_j^{SMB}t^*}{V(1-\varepsilon_k)} - \frac{\varepsilon_k}{1-\varepsilon_k} \tag{B.2}$$

In the relationship $a_1 < m_2 < m_3 < a_2$ [21], m_2 and m_3 can be replaced with the last equation. Each term of the inequality is multiplied by $(1-\varepsilon_k)$, and then ε_k is added:

$$(1-\varepsilon_k)a_1 + \varepsilon_k < \frac{Q_{II}^{SMB}t^*}{V} < \frac{Q_{III}^{SMB}t^*}{V} < (1-\varepsilon_k)a_2 + \varepsilon_k \tag{B.3}$$

At this point the following new variables r_j, g_k and h_k are introduced:

$$r_j = \frac{Q_j^{SMB}t^*}{V} \tag{B.4}$$

$$g_k = (1-\varepsilon_k)a_1 + \varepsilon_k \tag{B.5}$$

$$h_k = (1-\varepsilon_k)a_2 + \varepsilon_k \tag{B.6}$$

The new variables are placed in Eqs. (A.5)–(A.8) which gives the revised set of separation conditions:

$$h_k < r_I < \infty \tag{B.7}$$

$$g_k < r_{II} < r_{III} < h_k \tag{B.8}$$

$$0 < r_{IV} < g_k \tag{B.9}$$

where the particle porosity ε_p was assumed to be zero.

Appendix C. Identification of different separation regions in the r_{II}–r_{III} plot under linear conditions

The following mathematical derivations of different separation regions are based on the analytical solution of the ideal model [20], using four sections in the SMB unit. They assume that the separation conditions were not fulfilled during the cycle which just ended and that the rear of the concentration profile of component 1, the less retained one, is polluting the extract. This is due to the lower propagation velocity along a low-porosity column than along the other ones. So, during the first cycle of a superperiod, the velocity of component 1 in section II is too low and the rear of its profile cannot be pushed back past the feed node before the end of this cycle. It passes into section I at the end of the

cycle and elutes with the extract during the second cycle of the superperiod.

The propagation velocity of component 1 in section II, along column k, is given by the following equation:

$$w_{\mathrm{II},k} = \frac{Q_{\mathrm{II}}}{A[a_1(1-\varepsilon_k)+\varepsilon_k]} \tag{C.1}$$

This equation can be simplified by using Eqs. (20) and (21):

$$w_{\mathrm{II},k} = \frac{r_{\mathrm{II}}L}{g_k t^*} \tag{C.2}$$

The following relationship between the propagation velocities of the two feed components is valid with the assumption made above ($a_1 > 1$ and $\varepsilon_1 < \varepsilon_2$):

$$w_{\mathrm{II},1}(\varepsilon_1) < w_{\mathrm{II},2}(\varepsilon_2) \tag{C.3}$$

The length distance, $\Delta L_{\mathrm{C}}(1)$, between the rear of the concentration profile of component 1 and the feed node, when component 1 remains in section II at the end of the first cycle of the superperiod, can be calculated as

$$\Delta L_{\mathrm{C}}(1) = L - w_{\mathrm{II},1}t^* = L - \frac{r_{\mathrm{II}}L}{g_1} = L\left(1 - \frac{r_{\mathrm{II}}}{g_1}\right) \tag{C.4}$$

At the beginning of the second cycle, after the columns were switched, the remaining part of the profile front of component 1 is in section I. The column in section II is now a high-porosity column with a high propagation velocity. Under the following conditions, the rear of the profile of component 1 will leave section II at the end of this cycle and

$$w_{\mathrm{I},1}t_1 + w_{\mathrm{II},2}(t^* - t_1) \geq \Delta L_{\mathrm{C}}(1) + L \tag{C.5}$$

Assuming that $\Delta L_{\mathrm{C}}(1) = w_{\mathrm{I},1}t_1$ and using Eq. (C.2), this equation can be rewritten as

$$\frac{r_{\mathrm{II}}L}{g_2 t^*}\left(t^* - \frac{\Delta L_{\mathrm{C}}(1)}{r_{\mathrm{I}}L}g_1 t^*\right) \geq L \tag{C.6}$$

and thus

$$r_{\mathrm{II}}\left(1 - \left(L - \frac{r_{\mathrm{II}}}{g_1}L\right)\frac{g_1}{r_{\mathrm{I}}L}\right) \geq g_2 \tag{C.7}$$

Rearranging this equation leads directly to the following:

$$r_{\mathrm{II}}^2 + (r_{\mathrm{I}} - g_1)r_{\mathrm{II}} - g_2 r_{\mathrm{I}} \geq 0 \tag{C.8}$$

This equation has one positive solution, illustrated by the dotted line (1) in Fig. 3. If r_{II} is located within these boundaries the extract stream is polluted only during one of the four cycles.

Note that in this equation, g_1 (see Eq. (21)) is the highest of four possible boundary values g_k and corresponds to ε_1. The value g_2 is calculated for the column next to column 1 in the direction of the fluid flow. Although in the hypothetical case discussed here there are only two different porosities (i.e., $g_2 = g_3 = g_4$), the equations are derived for the general (and more realistic) problem of four different columns.

If component 1 does not leave section II at the end of the second cycle, the remaining distance towards the feed node can be determined by the following relationship:

$$\Delta L_{\mathrm{C}}(2) = L - w_{\mathrm{II},2}t^* = L - \frac{r_{\mathrm{II}}}{g_2}L\left(1 - \frac{g_1 - r_{\mathrm{II}}}{r_{\mathrm{I}}}\right) \tag{C.9}$$

Following the same algorithm, the required condition for the rear of the concentration profile of component 1 to be pushed back through the feed node into section III at the end of the third cycle is

$$w_{\mathrm{I},2}t_1 + w_{\mathrm{II},3}(t^* - t_1) \geq \Delta L_{\mathrm{C}}(2) + L \tag{C.10}$$

which can be simplified with the assumption that $\Delta L_{\mathrm{C}}(2) = w_{\mathrm{I},2}t_1$ and using Eq. (C.2):

$$\frac{r_{\mathrm{II}}L}{g_3 t^*}\left(t^* - \frac{\Delta L_{\mathrm{C}}(2)}{r_{\mathrm{I}}L}g_2 t^*\right) \geq L \tag{C.11}$$

and thus

$$r_{\mathrm{II}}\left(1 - \left(L - \frac{r_{\mathrm{II}}}{g_2}L\left(1 - \frac{g_1 - r_{\mathrm{II}}}{r_{\mathrm{I}}}\right)\right)\frac{g_2}{r_{\mathrm{I}}L}\right) \geq g_3 \tag{C.12}$$

If the inequality

$$r_{II}^3 + (r_I - g_1)r_{II}^2 + (r_I^2 - g_2 r_I)r_{II} - g_3 r_I^2 \geq 0 \quad \text{(C.13)}$$

is fulfilled, component 1 has left section II at the end of the third cycle. The dash-dotted line (2) represents this limit in Fig. 3.

If the rear of the concentration profile of component 1 still remains in section II at the end of the third cycle, it has to be pushed back during the fourth cycle in order to avoid instabilities of the process. Following the same algorithm, we find that the distance between the rear of the profile and the feed node is given by

$$\Delta L_C(3) = L - w_{II,3}t^* = L - \frac{r_{II}}{g_3}L\left(1 - \frac{\Delta L_C(2)g_2}{r_I L}\right) \quad \text{(C.14)}$$

and the separation condition is

$$w_{I,3}t_1 + w_{II,4}(t^* - t_1) \geq \Delta L_C(3) + L \quad \text{(C.15)}$$

This last equation can be rewritten as

$$\frac{r_{II}L}{g_4 t^*}\left(t^* - \frac{\Delta L_C(3)}{r_I L}g_3 t^*\right) \geq L \quad \text{(C.16)}$$

Inserting Eq. (C.2) in the previous equation and rearranging leads to

$$r_{II}^4 + (r_I - g_1)r_{II}^3 + (r_I^2 - g_2 r_I)r_{II}^2 + (r_I^3 - g_3 r_I^2)r_{II} - g_4 r_I^3 \geq 0 \quad \text{(C.17)}$$

If this condition is fulfilled by r_{II}, the rear of the band of component 1 will eventually be pushed back through the feed node during the last cycle of the superperiod, before the return of the odd column into section II. The dashed line (3) in Fig. 3 corresponds to this limit.

If the operating point is located to the left of this dashed line, the extract is polluted during all four cycles, to a different degree during each cycle. The rear end of the band of component 1 cannot be pushed back to the feed node during any cycle of a superperiod. However, as long as the operation point remains inside the triangle L0.7, the SMB process reaches a steady-state condition. The rear front of the band of component 1 does not penetrate further into section II. The higher flow-rate in section I prevents further pollution of the SMB system.

The same algorithm as was used in section II can be applied for the derivation of the similar conditions for section III of the SMB, when the front of the concentration profile of component 2 is polluting the raffinate stream. However, in this case a higher column porosity causes a lower rearward propagation velocity of the front of the profile of component 2.

Finally, the same algorithm can easily be extended to the case in which there are two or several columns in the section considered.

Note that only the positive real solutions of Eqs. (C.13) and (C.17) have been implemented.

References

[1] D.B. Broughton, C.G. Gerhold, US Pat. 2 985 589 (1961).
[2] D.M. Ruthven, C.B. Ching, Chem. Eng. Sci. 44 (1989) 1011.
[3] R.W. Neuzil, R.H. Jensen, in: Presented at AIChE Meeting, Philadelphia, PA, 1978, Paper 22.
[4] D.B. Broughton, R.W. Neuzil, J.M. Pharis, C.S. Brearley, Chem. Eng. Prog. 66 (1970) 70.
[5] E. Küsters, G. Gerber, F.D. Antia, Chromatographia 40 (1995) 387.
[6] A. Seidel-Morgenstern, C. Blümel, H. Kniep, in: F. Meunier (Ed.), Fundamentals of Adsorption, Vol. 6, Elsevier, Amsterdam, 1998, p. 303.
[7] M.P. Pedeferri, G. Zenoni, M. Mazzotti, M. Morbidelli, Chem. Eng. Sci. 54 (1999) 3735.
[8] D.C.S. Azevedo, L.S. Pais, A.E. Rodrigues, J. Chromatogr. A 865 (1999) 187.
[9] S. Khattabi, D.E. Cherrak, K. Mihlbachler, G. Guiochon, J. Chromatogr. A 893 (2000) 307.
[10] M. Negawa, F. Shoji, J. Chromatogr. 590 (1992) 113.
[11] C.B. Ching, B.G. Lim, E.J.D. Lee, S.C. Ng, J. Chromatogr. 634 (1993) 215.
[12] K. Hashimoto, Y. Shirai, S. Adachi, J. Chem. Eng. Jpn. 26 (1993) 52.
[13] B. Balannec, G. Hotier, in: G. Ganetsos, P.E. Barker (Eds.), Preparative and Production Scale Chromatography, Marcel Dekker, New York, 1993, p. 301.
[14] F. Charton, R.-M. Nicoud, J. Chromatogr. A 702 (1995) 97.
[15] H. Rhee, N.R. Amundson, Chem. Eng. Sci. 28 (1973) 55.
[16] G. Storti, M. Masi, S. Carra, M. Morbidelli, Chem. Eng. Sci. 44 (1989) 1329.
[17] G. Storti, M. Mazotti, M. Morbidelli, S. Carra, AIChE J. 39 (1993) 471.
[18] B.B. Fish, R.W. Carr, R. Aris, AIChE J. 39 (1993) 1783.
[19] T. Yun, Z. Bensetiti, G. Zhong, G. Guiochon, J. Chromatogr. A 758 (1997) 175.
[20] G. Zhong, G. Guiochon, Chem. Eng. Sci. 51 (1996) 4307.
[21] M. Mazotti, G. Storti, M. Morbidelli, J. Chromatogr. A 769 (1997) 3.
[22] B.J. Stanley, C.R. Foster, G. Guiochon, J. Chromatogr. A 761 (1996) 41.

[23] T. Yun, G. Zhong, G. Guiochon, AIChE J. 43 (1997) 935.
[24] R.-M. Nicoud, A. Seidel-Morgenstern, Isolation Purif. 2 (1996) 165.
[25] H. Guan, G. Guiochon, J. Chromatogr. A 731 (1996) 41.
[26] T. Yun, G. Zhong, G. Guiochon, AIChE J. 43 (1997) 2970.
[27] G. Guiochon, S.G. Shirazi, A.M. Katti, Fundamentals of Nonlinear and Preparative Chromatography, Academic Press, Boston, MA, 1994.
[28] C. Migliorini, M. Mazzotti, M. Morbidelli, AIChE J. 45 (1999) 1411.
[29] C. Migliorini, A. Gentilini, M. Morbidelli, Ind. Eng. Chem. Res. 38 (1999) 2400.
[30] M.S. Smith, G. Guiochon, J. Chromatogr. A 827 (1998) 241.
[31] C. Migliorini, M. Mazzotti, M. Morbidelli, J. Chromatogr. A 827 (1998) 161.